Direct numerical simulation of an oblique jet in a particle-laden crossflow

G. Agati, D. Borello, G. Camerlengo, F. Rispoli and J. Sesterhenn

1 Introduction

Jet in crossflow is a classic fluid dynamics problem widely studied in the last decades because of the big quantity of natural and industrial processes in which it is encountered [6]. The present study focuses on the interaction between solid suspended particles and gas turbines film cooling that is a commonly used coolant technique aiming at generating a protective film of cold fluid around the blade profile. Effective cooling systems are crucial to increase turbine inlet gas temperature and to protect turbine blade surfaces from the huge thermal stress generated. For this kind of application, to reduce the jet penetration into the crossflow, low values of jet to crossflow velocities and blowing ratio are generally adopted, with values generally ranging from 0.5 to 2 [1]. The blowing ratio (BR) is defined as the jet to the main flow mass flux ratio. In the jet in crossflow interaction, coherent vortex systems are generated in the zone of injection and, depending on the characteristic of the problem, dominate the phenomenon. When low values of BR are used the interaction of jets in crossflow is dominated by hairpin vortices ([10], [16]). Solid suspended particles are often encountered in the flow evolving in gas turbines due to sand ingestion when operating in hard environments or to the not complete hydrocarbon combustion (soot) [5]. Dispersed particles can deposit on gas turbines blades and vanes interacting with the cooling system and eventually provoking a reduction of its effectiveness [15]. As discussed in [13], particle deposition and entrainment in wall-bounded flows are strongly related to near-wall turbulent coherent structures.

G. Agati, D. Borello and F. Rispoli
Dipartimento di Ingegneria Meccanica e Aerospaziale, Università degli Studi di Roma La Sapienza, Via Eudossiana 18, 00184 Roma, Italy e-mail: {giuliano.agati,domenico.borello,franco.rispoli}@uniroma1.it

G. Camerlengo and J. Sesterhenn
Institut für Strömungmechanik und Technische Akustik, Technische Universität Berlin, Muller-Breslau-Str. 15, 10623 Berlin, Germany, e-mail: {gabriele.camerlengo,joern.sesterhenn}@tu-berlin.de

Because of the inherent complexity of the problem, a Direct Numerical Simulation of a 30° inclined cylindrical laminar jet issuing in particle-laden crossflow was performed.

2 Numerical and simulation details

The carrier fluid flow is described by means of skew-symmetric Navier-Stokes equations [9] discretized on a multi-block curvilinear grid illustrated in Fig. 1. Time integration is performed through a low-storage 4th order Runge-Kutta scheme while, as concerns the space discretization, a 6th order Summation By Parts finite difference scheme is adopted. The parallelization (MPI) is achieved by a hybrid approach using a multi-block code with a ghost layer synchronization as well as block internal decomposition into CPUs as explained in [14]. The dispersed phase is simulated by adopting a Lagrangian two-way coupling point-particle approach. In order to make computationally more efficient the particles tracing scheme, particle equation is solved in a uniform and orthonormal computational space different from the one where fluid flow equations are discretized. In this space, the algorithm tracing particles does not need iterative methods since an explicit correspondence exists between the coordinates of a point and the grid cell containing it. When the coupling between fluid and particle properties has to be accomplished, a given particle position in the c-space is transformed into its physical coordinate following the trilinear interpolation as suggested in [11]. Wall-particle interaction was also considered by adopting a generalized version ([4]) of the elasto-plastic impact/adhesion model firstly proposed by Thornton and Ning ([2], [3]). To obtain the desired circular section of the jet, porous media, acting as solid wall boundaries, were also included by means of a volume penalization method in the formulation presented in [12].

Jet in crossflow blowing ratio is set equal to 1, Mach number of the cross-flow is equal to 0.8, while the Reynolds number, based on the jet hole diameter and jet undisturbed velocity, is 3000. The cross-flow is initialized with a Blasius laminar boundary-layer with a $\delta_{99\%} = 1.32d$ at the jet exit center (being d the pipe jet diameter), while for the jet a fully developed laminar profile based on Hagen-Poiseuille flow is set along the pipe length as initial condition. Particles are injected

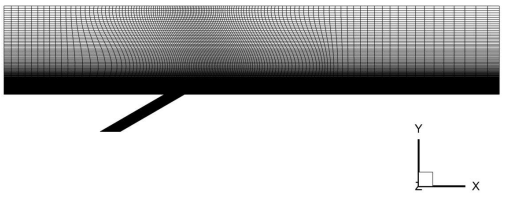

Fig. 1 Grid consists in about 542 mln grid points. Here it is shown in the symmetry plane and, for the sake of clarity, only one on eight points is plotted in all the dimensions. A grid clustering is performed in in the y- and x- directions.

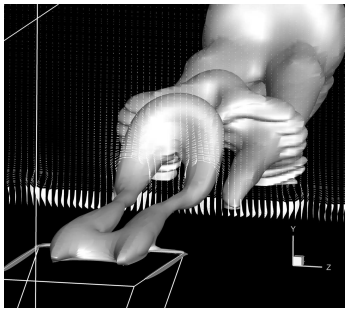

Fig. 2 Pressure isosurfaces are used to capture hairpin shaped vortices. Planar velocity vectors are represented on a transversal section.

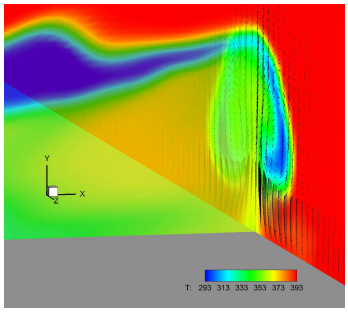

Fig. 3 Contour plot of temperature in the symmetry and in a cross-sectional plane where also velocity vectors indicating the presence of the CVP are drawn.

randomly distributed at the flat plate inlet section and a log-normal distribution is assumed to characterize particle diameters distribution with a count median diameter $CMD = 5\mu m$ and a geometric standard deviation $GSD = 1.6$ resulting in a mean value $d_m = 5.58\mu m$. Stokes particles number (St) ranges from 1 to 175.

3 Results and discussion

Instantaneous observation of the three-dimensional field demonstrated that, as expected, the fluid flow is dominated by hairpin shaped vortices shed periodically into the crossflow. As illustrated in Fig. 2 hairpin legs are associated to counter rotating vortex pairs (CVP) that persist in the far-field of the jet. These coherent structures influence temperature distribution (Fig. 3): hot air is entrained into the core of the jet resulting in some "hot spots" that can be observed along the wall surface.

In Fig. 4 (left) jet trajectory, defined as in [7], `i.e.` as the streamline originating from the center of the jet exit on the symmetry plane, is depicted. Jet trajectory presents a growing trend for the whole length of the flat plate even if jet penetration is always lower than $1.5d$. Jet temperature along its trajectory is also plotted in the same figure. Fig. 4 (right) shows the variation of film cooling effectiveness (Φ) on a line crossing the center of the bottom wall of the flat plate. Film cooling effectiveness is a commonly used dimensionless parameter to measure the quality of the cooling and it is defined as the gas-to-wall temperature difference over the gas-to-coolant temperature difference $\Phi = \frac{T_\infty - T_w}{T_\infty - T_c}$. After $x/d = 5$, Φ is less than 0.4, while for $x/d = 10$, $\Phi = 0.2$ and the jet influence on the crossflow temperature field can be considered negligible.

Particle spatial distribution is also strongly influenced by coherent fluid structures. Fig. 5 shows how a high concentration of particles is created on two symmetric regions extending along the lateral sides of hairpin vortices.

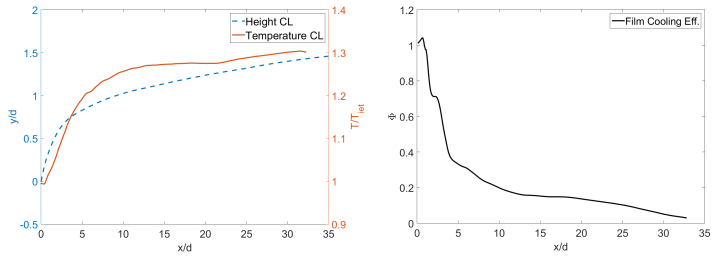

Fig. 4 On the left figure: trajectory and temperature variation along jet center-line. On the right figure: film cooling effectiveness on the center-line of the flat plate. Horizontal axis origin is here located on the center of jet pipe exit.

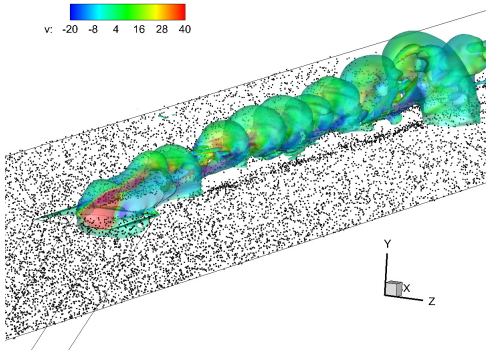

Fig. 5 Hairpin shaped vortices are coloured with vertical component of fluid velocity. Preferential concentration of particles is visible when plotting particles located in the region $y/d < 0.5$.

Following an analysis similar to [8], in Fig. 6 and in Fig. 7 particles are coloured by the wall-normal velocity. Smaller particles are captured by the counter rotating legs of hairpin vortices are transported toward the wall while particles hit by the head of the hairpins are pushed outward.

A similar behaviour can be also observed in Fig. 8 where a map of particle impacts on the bottom wall is shown. Statistics on particle impacts were carried out by means of probability density functions (PDFs) (not presented here). Only the 2% of the total number of impacts occurs in the zone upstream from the jet exit ($n_{imp} = 178$ in region α of Fig. 8). Downstream the jet, particles tend to impact on the wall along two symmetric sides of the jet exit for $z/d \approx \pm 1$ (regions γ). Particles impacting in these zones present lower values of dispersion of the Stokes number (*i.e.* lower standard deviation σ_{St}) and a mean value $St_m \simeq 19.68$. These are the particles that are trapped into fluid coherent structures and are transported toward the wall. In the external zones (regions β of Fig. 8), particles with a wider class of diameters impact the wall generally presenting bigger values of the St ($St_m = 37.64$). These particles

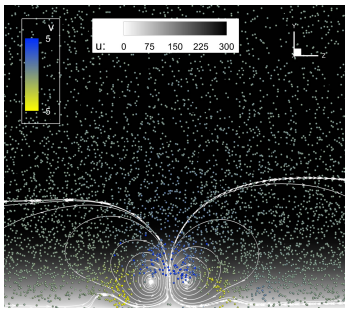

Fig. 6 Transversal section at $x = 8d$ from the jet exit. The contour plot and the planar streamlines are taken from the mean field.

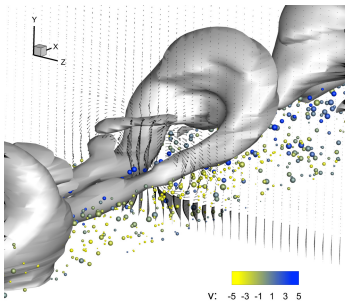

Fig. 7 Influence of CVP associated to hairpin legs on particle spatial distribution. Particles size varies with the *St* number.

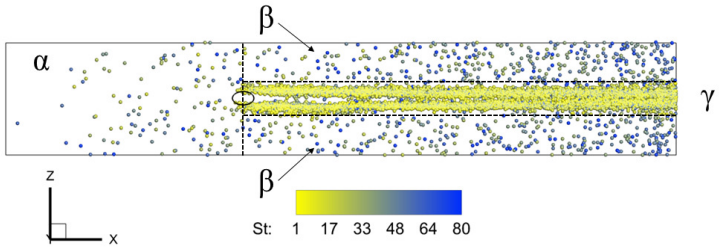

Fig. 8 Impact points on the wall coloured with particle Stokes number.

are subject to the effect of the CVP but do not fully follow vortices due to stronger inertia effects. Statistics carried out are summarized in Tab. 1.

Table 1 Statistics on particle impacts on the wall for the different regions illustrated in Fig. 8.

Regions	$\mathbf{n_{imp}}$	$\mathbf{St_m}$	$\boldsymbol{\sigma_{St}}$
Overall	9794	22.34	16.04
Region α	178	36.96	24.25
Region β	1329	37.64	21.90
Region γ	7547	19.68	12.89

4 Conclusions

A DNS of a jet in a particle-laden crossflow was performed. As expected, the fluid flow is dominated by hairpin vortices shed periodically from the pipe into the crossflow. The hairpin legs are counter-rotating and this streamwise vorticity has a strong

influence on temperature distribution and induces a preferential concentration on the dispersed phase field. Spatial distributions characterizing the impact regions were computed. Downstream from the jet exit particles characterized by low values of the St number tend to impact the wall in two symmetric sides of the jet exit for $z/d = \pm 1$ while in the external regions particles with higher values of St more probably impact the wall.

Acknowledgements We acknowledge the CINECA award under the ISCRA initiative, for the availability of high performance computing resources and support.

References

1. Acharya, S., Tyagi, M., Hoda, A. : Flow and Heat Transfer Predictions for Film Cooling, Annals of the New York Academy of Sciences, **934**, 110–125 (2001)
2. Agati, G., Borello D., Rispoli, F., Venturini, P.: An Innovative Approach to Model Temperature Influence on Particle Deposition in Gas Turbines. ASME Turbo Expo: Power for Land, Sea, and Air, Volume 5C: Heat Transfer (2016)
3. Borello, D. and Rispoli, F. and Venturini, P. : An integrated particle-tracking impact/adhesion model for the prediction of fouling in a subsonic compressor, **134**(9) (2012)
4. Camerlengo, G. and Borello, D. and Salvagni, A. and Sesterhenn, J. : DNS Study of Dust Particle Resuspension in a Fusion Reactor Induced by a Transonic Jet into Vacuum, Flow Turbulence Combustion, **101**(1), 101–247 (2018)
5. Lefebvre, A. H. and Ballal, D. R., Gas Turbine Combustion: Alternative Fuels and Emissions, Third Edition, CRC Press, (2010)
6. Mahesh, K. : The Interaction of Jets with Crossflow, Annual Review of Fluid Mechanics, **45**(1), 379–407 (2013)
7. Muppidi, S. and Mahesh, K. : Study of trajectories of jets in crossflow using direct numerical simulations, Journal of Fluid Mechanics, **530**, 81–100 (2005)
8. Prevel, M. and Vinkovic,I. and Doppler, D. and Pera, C. and Buffat, M.: Direct numerical simulation of particle transport by hairpin vortices in a laminar boundary layer, International Journal of Heat and Fluid Flow, **43**, 2–14 (2013)
9. Reiss, J. and Sesterhenn, J. : A conservative, skew-symmetric Finite Difference Scheme for the compressible Navier–Stokes Equations, Computers & Fluids, **101**, 208–219 (2014)
10. Sau, R. and Mahesh, K.: Dynamics and mixing of vortex rings in crossflow, Journal of Fluid Mechanics, **604**389–409 (2008)
11. Schafer, F. and Breuer, M., Comparison of c-space and p-space particle tracing schemes on high-performance computers: accuracy and performance, International Journal for Numerical Methods in Fluids, **39**(4), 277–299, (2002)
12. Schulze, J. and Sesterhenn, J., Optimal distribution of porous media to reduce trailing edge noise, Computers & Fluids, **78**, 41–53 (2013)
13. Soldati, A. and Marchioli, C., Physics and modelling of turbulent particle deposition and entrainment: Review of a systematic study, International Journal of Multiphase Flows, **35**, 827–839 (2009)
14. Stein, L. and Sesterhenn, J., An acoustic model of a Helmholtz resonator under a grazing turbulent boundary layer Acta Mechanica, **230**(6), 2013–2029 (2019)
15. Lawson, S.A. and Thole, K.A. : Effects of Simulated Particle Deposition on Film Cooling, Journal of Turbomachinery, **133**(2) (2010)
16. Tyagi, M. and Acharya, S.: Large eddy simulation of film cooling flow from an inclined cylindrical jet, Journal of Turbomachinery, **125**(4), 734–742 (2003)